

Deconfined criticality critically defined

T. SENTHIL¹, Leon BALENTS², Subir SACHDEV³,
Ashvin VISHWANATH¹, and Matthew P. A. FISHER⁴

¹*Department of Physics, Massachusetts Institute of Technology, Cambridge MA 02139*

²*Department of Physics, University of California, Santa Barbara CA 93106-4030*

³*Department of Physics, Yale University, P.O. Box 208120, New Haven CT 06520-8120*

⁴*Kavli Institute for Theoretical Physics, University of California, Santa Barbara, CA 93106-4030*

We describe characteristic physical properties of the recently introduced class of deconfined quantum critical points. Using some simple models, we highlight observables which clearly distinguish such critical points from those described by the conventional Landau-Ginzburg-Wilson framework: such a distinction can be made quite precisely even though both classes of critical points are strongly coupled, and neither has sharp quasiparticle excitations. We also contrast our classification from proposals by Bernevig *et al.* and Yoshioka *et al.*

Proceedings of the International Conference on Statistical Physics of Quantum Systems -- novel orders and dynamics, July 17–20, 2004, Sendai, Japan

KEYWORDS: antiferromagnet, valence bond solid, spin liquid, gauge theory, topological order

1. Introduction

A major focus of the study of correlated electron systems has been the analysis of continuous quantum phase transitions in two spatial dimensions. These are described by quantum field theories in 2+1 spacetime dimensions, and the most interesting are strongly-coupled: this means that there is no formulation of the critical theory in terms of free boson or fermion fields. (Indeed no such free field description is known for a wide variety of interesting critical points in 2 + 1 dimensions, and most probably simply does not exist). Rather, the gapless critical excitations interact with each other with a coupling of order unity. In contrast, in 1+1 dimensions it is often the case that there is a preferred formulation of the critical theory in terms of free fields. In the absence of such a free field formulation, there is no direct and simple physical interpretation of the excitation spectrum of 2+1 dimensional critical points, and of the interactions between the excitations.

Nevertheless, a great deal of understanding of some 2+1 dimensional critical points has been achieved by what may be called the Landau-Ginzburg-Wilson (LGW) framework.¹ In the LGW approach one identifies the order parameter (denoted φ) and elementary excitations

(usually, fluctuations of φ) characterizing the phases adjacent to the critical point; then, as we review below, a sophisticated renormalized perturbation theory of the interactions between φ excitations can be developed to also describe the spectrum of the quantum critical point.

In recent work,² we have argued that there are certain 2+1 dimensional critical points which do not fall into the above LGW framework. For these critical points, the best starting point for a description of the critical theory is not the order parameter, but an emergent set of fractionalized excitations which are special only to the critical point, and not present in either phase adjacent to the critical point. Moreover, there is an additional *topological structure* present at the critical point, connected with a topological conservation law. The extra conserved quantity is conveniently interpreted as the total flux of a gauge field that emerges at the critical point. This total flux is conserved only asymptotically at low energies at the quantum critical point. This conservation law provides a sharp distinction between these *deconfined* critical points and the conventional LGW critical points (for which there is no such conservation law). We will review an example of such a deconfined critical point below.

We strongly emphasize that the phenomena displayed near the quantum critical points we have dubbed deconfined are strikingly different from those near more conventional (even if strongly interacting) ones. Thus the nomenclature ‘deconfined’ has physical content, and is not just a matter of imposing terminology on some familiar and well-understood critical phenomena. Indeed, not all strongly interacting critical points are to be regarded as deconfined.

In earlier work, Laughlin³ had proposed fractionalization at 2+1 dimensional critical points on phenomenological grounds. However, the specific implementation of his scenario by Bernevig, Giuliano, and Laughlin⁴ disagrees with the classification we have proposed above. Indeed the example considered - the usual $O(n)$ critical point in $2 + 1$ dimensions, the field theory in Eq. (2.4) below - is universally accepted as the canonical example of LGW criticality, including by Bernevig *et al.*⁴ Despite this, Bernevig *et al.*⁴ predicted “a new spectroscopic effect that should occur very generally at quantum phase transitions described by $O(n)$ σ -models”—the existence of “excitations similar to meson resonances” of fractionalized spin $S = 1/2$ “elementary excitations with integrity analogous to spinons”. As discussed in Section 2, for the usual $O(n)$ critical point as described by Eq. (2.4), the spectrum⁵ near the phase transition can be fully understood in terms of the renormalized perturbation theory of $S = 1$ φ excitations, and it does not display any signatures of fractionalized $S = 1/2$ spinon-like excitations at any length scale. In particular, the resonances predicted by Bernevig *et al.* simply do not exist in this model. Moreover, if such resonances are found for a particular model which exhibits a quantum critical point in this universality class, they must be ascribed to non-universal (usually) lattice scale phenomena unrelated to the universal critical singularities associated with the phase transition.

An example of our deconfined critical points is reviewed in Section 3: it is described by the critical quantum field theory in Eq. (3.2) of $S = 1/2$ complex spinors z_a and a non-compact $U(1)$ gauge field A_μ . The presence of the gauge field, and the associated ‘photon’-like excitations, is a consequence of the topological conservation law at the critical point. A key point is that this field theory applies at all length scales (much larger than the lattice spacing) only at the quantum critical point. Away from the critical point, there is a very large length scale (much larger than the usual order parameter correlation length) beyond which ‘dangerously irrelevant’ corrections eventually dominate, and lead to the loss of the topological conservation law. The fractionalized degrees of freedom that rear their head at the critical point also undergo confinement by this scale. The presence of this second very large length scale is an important secondary characteristic of our deconfined critical points.

On a different note, we also strongly emphasize that the occurrence of deconfined quantum critical points does not in the least imply that fractionalized excitations are *necessarily* associated with quantum criticality in $2 + 1$ dimensional strongly correlated systems (other than in the fractional quantum Hall effect). Indeed, a large body of solid theoretical work over the last several years has established the stability of quantum *phases* of matter in two or higher dimensions where the excitations have fractional quantum numbers. These higher dimensional fractionalized phases, and the deconfined quantum critical points, have in common the presence of extra topological structure absent in the microscopic models in which they arise. This structure is associated with the presence of new topological conservation laws that are useful characterizations of the deconfinement. The corresponding conserved quantities can fruitfully be viewed as the fluxes of appropriate deconfined gauge fields.

We will present examples of a LGW and a deconfined critical point in the following two sections, and contrast their properties. A simple example of a LGW critical point, presented in Section 2, is provided by lattice models of $O(n)$ quantum rotors. These display second order quantum phase transitions between ordered phases where the $O(n)$ symmetry is broken, and simple disordered phases which preserve all the symmetries of the microscopic Hamiltonian. The phase transition is in the universality class of the usual $O(n)$ model in $2+1$ dimensions (and is described by the continuum $O(n)$ non-linear sigma model field theory in Eqs. (1.5) and (2.4)). A more sophisticated microscopic situation, presented in Section 2.1, which displays a quantum transition in the same universality class is a model of spin-1/2 quantum Heisenberg spins on a ‘dimerized’ lattice. In all these cases the transition is well-described within the standard LGW paradigm. Indeed this paradigm was evolved in the specific context of these universality classes - albeit viewed as thermal phase transitions in three dimensions. In contrast to this situation, our deconfined critical points,² reviewed in Section 3, display strikingly different phenomena. We will review one example - namely the transition between Néel and valence bond solid ordered phases of spin-1/2 square lattice quantum antiferromagnets - that

aply illustrates the breakdown of the LGW paradigm.

The following discussion in this section presents characteristics of the phase transition which apply in *both* the LGW and deconfined cases.

One of the phases beside both phase transitions is characterized by the non-zero expectation value of the Néel order parameter φ_α ($\alpha = x, y, z$), representing the component of the staggered spin polarization at an ordering wavevector \mathbf{K} . We tune the system across the quantum phase transition by varying a coupling g . For $g < g_c$, the ground state has Néel order and hence

$$\langle \varphi_\alpha \rangle \neq 0 \quad ; \quad g < g_c, \text{ Néel state.} \quad (1.1)$$

The quantum critical point of interest is at $g = g_c$, and for $g > g_c$ SU(2) spin rotation invariance is restored and we have the paramagnetic ground state:

$$\langle \varphi_\alpha \rangle = 0 \quad ; \quad g > g_c, \text{ paramagnetic state.} \quad (1.2)$$

In both the cases we consider below, the paramagnetic state has a sharp $S = 1$ excitation which can be interpreted as the oscillations of the order parameter φ_α about its zero mean value in Eq. (1.2). This implies that the susceptibility of φ_α autocorrelations, χ_φ , has the following form at small frequencies (ω) and wavevectors (k):

$$\text{Im} [\chi_\varphi(k, \omega)] \sim \frac{Z}{\Delta} \delta(\omega - \Delta - \mathcal{O}(k^2)) + \dots \quad ; \quad g > g_c. \quad (1.3)$$

Here Δ is the spin gap above which the $S = 1$ excitation has a quadratic dispersion, and Z is the quasiparticle residue. The low energy spinful excitations of the paramagnet therefore have a simple quasiparticle interpretation.

Now let us consider the spectrum at the critical point $g = g_c$. Both critical points described below have an effective ‘relativistic’ invariance and the critical susceptibility has the form

$$\chi_\varphi(k, \omega) \sim \frac{1}{(c^2 k^2 - \omega^2)^{1-\eta/2}} \quad ; \quad g = g_c, \quad (1.4)$$

where the exponent η is anomalous dimension of the φ_α field, and c is a velocity. Note that because $\eta \neq 0$, the imaginary part of Eq. (1.4) does not have quasiparticle delta-function, but only a continuum contribution for $\omega > ck$. So, clearly, there are no $S = 1$ quasiparticle excitations at the quantum critical point. This absence of quasiparticles is a general property of strongly-coupled quantum critical points.

In Section 2, we will argue that in many cases the continuum spectral density in Eq. (1.4) can be understood in LGW theory by an evolution from the quasiparticle spectral density in Eq. (1.3) (contrary to claims by Bernevig *et al.*⁴). We can use perturbative renormalization group techniques to analyze the consequences of interactions between the $S = 1$ quasiparticle excitations. As we approach the critical point with $g \searrow g_c$, these interactions lead⁵ to a decrease in Z until it vanishes at $g = g_c$, and the spectral density takes the non-quasiparticle

form in Eq. (1.4). The magnitude of the anomalous dimension η is usually small in such an approach, and this underlies the success of the perturbative approach.

Section 3 will turn to the novel deconfined critical points. The forms in Eqs. (1.1), (1.2), (1.3), and (1.4) continue to apply in this case too. So the critical spectrum in Eq. (1.4) is present in both the LGW and deconfined cases, and is *not* an indicator of fractionalization by itself. However in the deconfined case, the underlying theory of the excitations leading to the response function in Eq. (1.4) is different, and expressed in terms of fractionalized modes. A sharp observable distinction between the two cases lies in the emergence of a new conservation law at the critical point. The topological flux is defined (in the continuum limit) by

$$\mathcal{Q} = \frac{1}{4\pi} \int dx dy \epsilon_{\alpha\beta\gamma} \varphi_\alpha \partial_x \varphi_\beta \partial_y \varphi_\gamma, \quad (1.5)$$

(here, we have rescaled φ_α to be a unit vector—details in the sections below) and measures the skyrmion number⁶ of the spin configuration. \mathcal{Q} is conserved only at the $g = g_c$ deconfined critical point, and not at other values of g . It is also not conserved at *any* value of g for the LGW case discussed in Section 2. The conservation of \mathcal{Q} signifies the emergence of an extra global $U(1)$ symmetry at the deconfined critical point, and the presence of an additional set of gapless gauge excitations. A secondary consequence is that it naturally leads to larger values of the exponent η in Eq. (1.4) for deconfined critical points.

2. LGW criticality

Consider a lattice model of $O(n)$ quantum rotors. The $n = 2$ case is well-studied in the context of superconductor-insulator transitions in Josephson junction arrays. The $n = 3$ case describes quantum phase transitions in certain classes of quantum antiferromagnets. This class of models has been regarded as prototypical of quantum phase transitions (in much the same way as the classical $O(n)$ models are prototypes of thermal phase transitions). Here we will briefly review their properties. This will set the stage to appreciate the novel and unusual phenomena near the deconfined quantum critical points.

For concreteness, we specialize to the case $n = 3$.

$$H = g \sum_r \frac{\vec{L}_r^2}{2} - \frac{1}{g} \sum_{\langle rr' \rangle} \hat{n}_r \cdot \hat{n}_{r'} \quad (2.1)$$

Here \hat{n}_r is a three component unit vector on the sites r of a square lattice. The vector operator \vec{L}_r is the corresponding angular momentum which generates rotations of \hat{n}_r . For small g the second ‘potential’ term in the Hamiltonian dominates and the \hat{n} vector orders:

$$\langle \hat{n}_r \rangle \neq 0 \quad (2.2)$$

The $O(3)$ symmetry of the Hamiltonian H is then spontaneously broken down to $O(2)$. The low energy excitations are simply two linearly dispersing ‘spin waves’ as required by Goldstone’s theorem. For large g , on the other hand, the first term dominates. In this case the ground state

is a paramagnet which preserves all the symmetries of the Hamiltonian. (A simple caricature of the ground state is obtained by putting each rotor in the $\vec{L}_r^2 = 0$ state.) The low energy excitations about this state are now gapped and simply correspond to a massive triplet of spin-1 bosons.

Upon increasing g there is a quantum phase transition between these two phases. The crucial conceptual idea behind the description of this transition is that all the universal critical singularities are due to the long wavelength long time fluctuations of the order parameter field \hat{n} . This idea (which can ultimately be traced to Landau) underlies all of our understanding of phase transitions. A suitable continuum theory that describes these fluctuations is indeed the $O(3)$ non-linear sigma model field theory in $2 + 1$ dimensions:

$$\mathcal{S}_{\text{nlsm}} = \int d^2x d\tau \frac{1}{2g} \left[(\partial_x \hat{n})^2 + (\partial_y \hat{n})^2 + \frac{1}{c^2} (\partial_\tau \hat{n})^2 \right] \quad (2.3)$$

Equivalently, we may soften the unit vector constraint on \hat{n} by letting $\hat{n} \sim \vec{\varphi}$ and study a ‘soft-spin’ version of the same theory which has the same universal critical properties:

$$\mathcal{S}_\varphi = \int d^2r d\tau \left[\frac{1}{2} \left\{ (\partial_\tau \varphi_\alpha)^2 + c^2 (\partial_x \varphi_\alpha)^2 + c^2 (\partial_y \varphi_\alpha)^2 + s \varphi_\alpha^2 \right\} + \frac{u}{24} (\varphi_\alpha^2)^2 \right]. \quad (2.4)$$

Here we have rescaled φ_α to fix the co-efficient of the temporal gradient term at unity, and the quantum critical point is tuned by varying s ; in mean-field theory $s \sim g - g_c$.

It is a simple matter to explore the spectrum of excitations in $g < g_c$ and $g > g_c$ phases in powers of u . The results are identical in form to those obtained above for the lattice Hamiltonian. For $g < g_c$ we obtain a doublet of spin wave modes with linear dispersion, while for $g > g_c$ we obtain a triplet of φ_α oscillations about $\varphi_\alpha = 0$ with a non-zero energy gap.

The analysis of \mathcal{S}_φ at $g = g_c$ requires a somewhat more sophisticated approach. We use the fact that the field theory \mathcal{S}_φ is actually a familiar and well-studied model in the context of classical critical phenomena. Upon interpreting τ as a third spatial co-ordinate, \mathcal{S}_φ becomes the theory of a classical $O(3)$ -invariant Heisenberg ferromagnet at finite temperatures. The Curie transition of the Heisenberg ferromagnet then maps onto the quantum critical point between the paramagnetic and Néel states described above. A number of important implications for the quantum problem can now be drawn immediately.

First, the structure of the renormalization group flows that describe the critical fixed point is well-known. The critical fixed point has precisely one relevant perturbation (which describes the parameter tuning the system through the transition). The flow away from the critical fixed point ultimately ends in stable fixed points that characterizes either of the two phases. There is a *single* diverging length scale on approaching the transition. For instance, on the paramagnetic side this may simply be taken to be the spin correlation length. Associated with this there is a single diverging time scale - or equivalently a vanishing energy scale.

Again, on the paramagnetic side this may be taken to be the gap to the triplon excitations. The theory \mathcal{S}_φ has a ‘relativistic’ invariance, and consequently the dynamic critical exponent must be $z = 1$. The critical fixed point may be accessed in controlled expansions in $3 - \epsilon$ dimensions or directly in $d = 2$ in an $1/n$ expansion. Excellent numerical results for a variety of universal properties are also available.

The spin correlation length will diverge at the quantum critical point with the exponent⁷ $\nu = 0.7048(30)$. The spin gap of the paramagnet, Δ , vanishes as $\Delta \sim (g - g_c)^{z\nu}$, and this prediction is in excellent agreement with numerical studies of the model H_d in Eq. (2.6) below.⁸

A somewhat more non-trivial consequence of the mapping to the classical three dimensional problem is in the structure of the spectrum at the critical point $g = g_c$. At the Curie transition of the classical ferromagnet it is known¹ that spin correlations decay as $\sim 1/p^{2-\eta}$, where p is the 3-component momentum in the 3-dimensional classical space. We can now analytically continue this expression from its p_z dependence in the third classical dimension to the real frequency, ω , describing the quantum antiferromagnet. This immediately yields the general result Eq. (1.4); the imaginary part of the dynamic susceptibility has the form

$$\text{Im}\chi_\varphi(k, \omega) \sim \text{sgn}(\omega) \sin\left(\frac{\pi\eta}{2}\right) \frac{\theta(|\omega| - c|k|)}{(\omega^2 - c^2k^2)^{1-\eta/2}} \quad (2.5)$$

where θ is the unit step function. As expected, there are no quasiparticles at the critical point, and only a dissipative critical continuum.

On moving away from the critical point - say into the paramagnetic phase - the spectrum crosses over into that characteristic of the paramagnetic fixed point at a scale set by the energy gap Δ . There is a delta-function pole in the dynamic susceptibility as in Eq. (1.3), and additional universal structure at higher frequencies. Indeed (at zero momentum) the *only* scale for the frequency in the universal scaling limit is Δ . The presence of this single scale implies that there can be no structure (such as resonances) in the spectral function that have width that is parametrically smaller than their energy - hence there is no real sharp meaning that can be given to statements about the existence of ‘spinons’ with integrity near this kind of quantum phase transition.

The key point of this section is to note that the critical results in Eqs. (1.4) and (2.5) can be understood entirely within the framework of the LGW theory, as presented *e.g.* in the book by Ma.¹ We set up a renormalization group analysis in powers of u , and then compute the correlators of the critical theory by a renormalized perturbative analysis of the renormalization group fixed point. The only additional subtlety is the analytic continuation to real frequencies, and this is aided by the relativistic invariance of the underlying theory, as we have seen above.

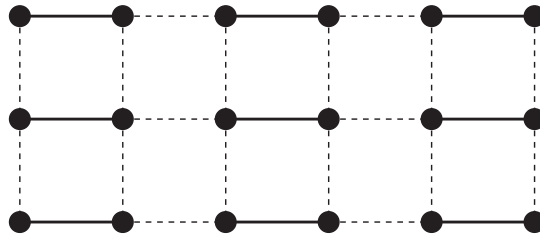


Fig. 1. The coupled dimer antiferromagnet. Spins ($S = 1/2$) are placed on the sites, the \mathcal{A} links are shown as full lines, and the \mathcal{B} links as dashed lines.

2.1 Coupled dimer antiferromagnet

To see how a transition in the universality class described above may arise in quantum antiferromagnets of spin-1/2 Heisenberg moments on two dimensional lattices, it is instructive to consider the following the “coupled dimer” Hamiltonian⁹ (more detail may be found in another recent review by one us¹⁰):

$$H_d = J \sum_{\langle ij \rangle \in \mathcal{A}} \mathbf{S}_i \cdot \mathbf{S}_j + \frac{1}{g} J \sum_{\langle ij \rangle \in \mathcal{B}} \mathbf{S}_i \cdot \mathbf{S}_j \quad (2.6)$$

where \mathbf{S}_j are spin-1/2 operators on the sites of the coupled-ladder lattice shown in Fig 1, with the \mathcal{A} links forming decoupled dimers while the \mathcal{B} links couple the dimers as shown. The ground state of H_d depends on the dimensionless coupling g , and we will restrict our attention to $J > 0$ and $g \geq 1$. Exactly at $g = 1$, H_d is the familiar square lattice antiferromagnet which describes La_2CuO_4 . The $g > 1$ regime has a structure similar to models used to describe Mott insulators like TlCuCl_3 :^{11–13} in this case, the value of g has been tuned across the quantum critical point by applied pressure.¹³

We will see that the phases and phase transitions of this model are well represented by the $O(3)$ quantum rotor model discussed above. Indeed the present lattice model provides a sophisticated example of a phase transition that fits in well with the LGW paradigm. This important conclusion disagrees with a recent claim by Yoshioka *et al.*¹⁴ of “deconfinement” in a coupled dimer antiferromagnet which differs only slightly from Eq. (2.6). We also note that the description of coupled dimer antiferromagnets by LGW criticality is strongly supported by numerical studies.⁸

Let us first consider the case where g is close to 1. Exactly at $g = 1$, H_d is known to have long-range, magnetic Néel order in its ground state *i.e.* the spin-rotation symmetry is broken and Eq. (1.1) holds with

$$\varphi_\alpha(\mathbf{x}_j) = \eta_j S_{j\alpha} \quad (2.7)$$

where $\eta_j = e^{i\mathbf{K} \cdot \mathbf{x}_j} = \pm 1$ with the ordering wavevector $\mathbf{K} = (\pi, \pi)$. This long-range order is expected to be preserved for a finite range of g above 1. The low-lying excitations above the ground state consist of slow spatial deformations in the orientation $\langle \varphi_\alpha \rangle$: these are the familiar

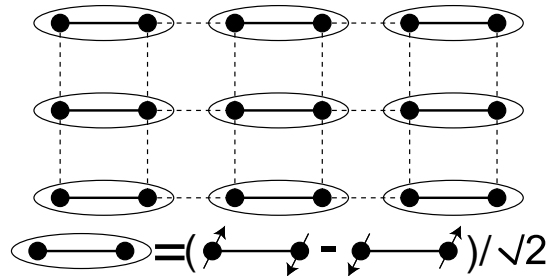


Fig. 2. Schematic of the quantum paramagnet ground state for $g \rightarrow \infty$. The ovals represent singlet valence bond pairs.

spin waves, a standard small fluctuation analysis yields *two* polarizations of spin waves at each wavevector $\mathbf{k} = (k_x, k_y)$ (measured from \mathbf{K}), and they have excitation energy

$$\varepsilon_k = (c_x^2 k_x^2 + c_y^2 k_y^2)^{1/2}, \quad ; \quad g < g_c \quad (2.8)$$

where the spatial anisotropy of the model now requires distinct spin-wave velocities, c_x, c_y , in the two spatial directions.

Let us turn now to very large g . Exactly at $g = \infty$, H_d is the Hamiltonian of a set of decoupled dimers, with the simple exact ground state wavefunction shown in Fig 2: the spins in each dimer pair into valence bond singlets, leading to a paramagnetic state which preserves spin rotation invariance and all spatial symmetries of the Hamiltonian H_d . Excitations are now formed by breaking a valence bond, which leads to a *three*-fold degenerate state with total spin $S = 1$, as shown in Fig 3a. At $g = \infty$, this broken bond is localized, but at small but finite $1/g$ it can hop from site-to-site, leading to a triplet quasiparticle excitation. Note that this quasiparticle is *not* a spin-wave (or equivalently, a ‘magnon’) but is more properly referred to as a spin 1 *exciton* or a *triplon*.¹⁵ Indeed this excitation is the exact analog of the gapped triplet boson in the paramagnetic phase of the quantum rotor model. We parameterize its energy at small wavevectors k (measured from the minimum of the spectrum in the Brillouin zone) by

$$\varepsilon_k = \Delta + \frac{c_x^2 k_x^2 + c_y^2 k_y^2}{2\Delta}, \quad ; \quad g > g_c \quad (2.9)$$

where Δ is the spin gap, and c_x, c_y are velocities. A simple perturbative calculation in $1/g$ shows that the φ_α susceptibility has the form postulated in Eq. (1.3).

Fig 3 also presents a simple argument which shows that the triplon cannot fission into two $S = 1/2$ ‘spinons’, and so the delta function in Eq. (1.3) is the first non-vanishing contribution to the spectral density at low energies. For the particular quantum phase transition discussed in the present Section, it is legitimate to entirely neglect this meson-like structure of the triplon consisting of a quark-antiquark pair of spinons. In particular, the ‘confinement’ length scale below which this structure is apparent stays finite on approaching the transition. As such,

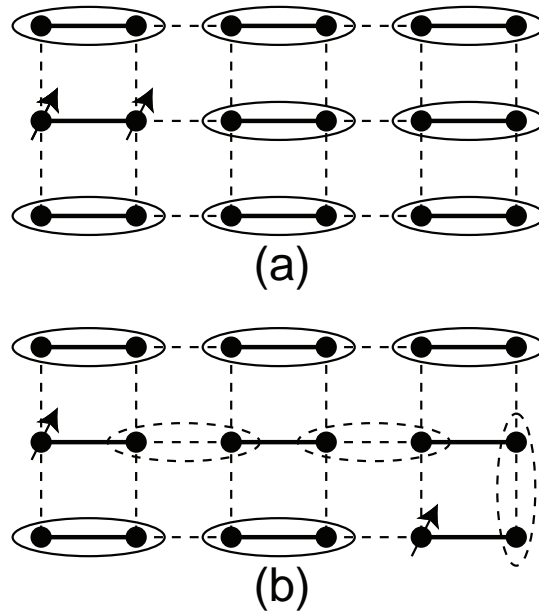


Fig. 3. (a) Cartoon picture of the bosonic $S = 1$ excitation of the paramagnet. In the LGW approach, this excitation is a quantum of oscillation of φ_α about $\varphi_\alpha = 0$. (b) Fission of the $S = 1$ excitation into two $S = 1/2$ spinons—these are the z_α quanta of Section 3. The spinons are connected by a “string” of valence bonds (denoted by dashed ovals) which lie on weaker bonds; this string costs a finite energy per unit length and leads to the confinement of spinons. It is important to note that this stringy structure, and associated excitations, is *absent* from the φ_α field theory in Eq. (2.4), contrary to the claim by Bernevig *et al.*⁴ In this lattice spin model the “existence” of spinons is a non-universal lattice scale effect, entirely unrelated to the universal long length scale singularities governed by the nearby quantum critical point. By contrast, near the deconfined critical points of Section 3, the stringy structure mediating spinon interactions is present at arbitrarily long length scales, being controlled by the universal critical fluctuations. But these are not described by the $O(3)$ sigma model field theory of Eqs. (2.3) and (2.4).

the “existence” of spinons and their confining interaction in this model are non-universal lattice scale effects, physically unrelated to the critical fluctuations that control the universal properties of the phase transition. In effect, the present section contains a ‘chiral model’ field theory of the mesons alone, which contains no signature of the quark-like spinons, contrary to claims by Bernevig *et al.*⁴ Moreover, since the LGW theory describes the universal critical properties of the coupled dimer system, any signatures of such lattice-scale spinons that might obtain in a particular model will *disappear* in the vicinity of its critical point. By contrast, in the examples of deconfined criticality discussed later, the confinement length scale will also diverge on approaching the transition. It will then be necessary to include the spinon structure of the triplon in the paramagnet in studying the transition. We will discuss how to do this in Section 3.

The very distinct symmetry signatures of the ground states and excitations between $g \gtrsim 1$

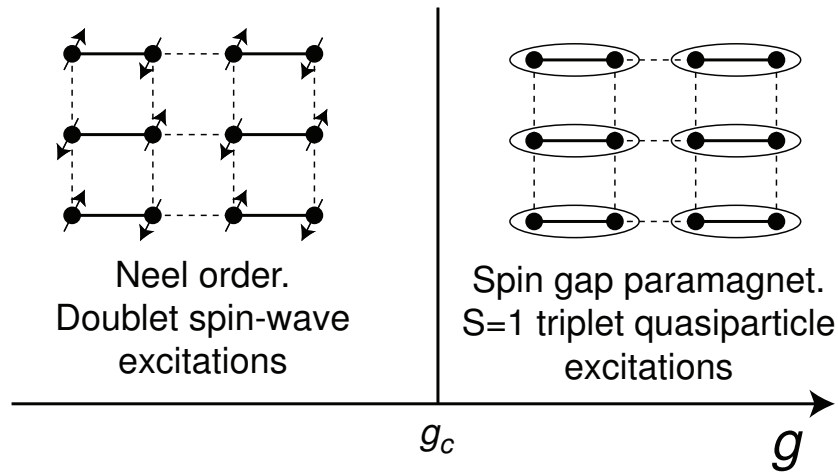


Fig. 4. Ground states of H_d as a function of g . The quantum critical point is at⁸ $1/g_c = 0.52337(3)$. The compound TlCuCl_3 undergoes a similar quantum phase transition under applied pressure¹³ which acts to decrease the value of g .

and $g \rightarrow \infty$ make it clear that the two limits cannot be continuously connected. It is known that there is an intermediate second-order phase transition at^{8,9} $1/g_c = 0.52337(3)$ between these states as shown in Fig 4.

A quantum field theory for the quantum critical point at $g = g_c$ can be derived microscopically,¹⁰ but here we guess the answer by following the canonical LGW procedure. We focus on the order parameter φ_α , and write down the most general effective action in powers of φ_α consistent with lattice space group, spin rotation, and time reversal symmetries. Such a procedure yields the familiar φ^4 field theory in 2+1 dimensions with the action Eq. (2.4) (a simple spatial rescaling absorbs the anisotropic spin-wave velocities $c_{x,y}$). Thus as far as universal critical properties are concerned we can simply take over the discussion provided above in the context of the rotor model.

3. Deconfined criticality

In contrast to the conventional picture described in the previous section, recent work² has discussed a number of examples of quantum critical points which display very different phenomena. These violate various aspects of the conventional LGW theory. Here we will illustrate these differences in the context of a specific example - namely a quantum phase transition between Néel and valence bond solid ordered phases of spin-1/2 Heisenberg moments on an *isotropic* two dimensional lattice.

The Néel phase breaks spin rotation symmetry, is well-known, and needs little further description here. The valence bond solid (VBS) phase is a paramagnet that has some similarities with the paramagnet in the coupled dimer Hamiltonian of Section 2.1. However on the isotropic square lattice, the valence bond solid state *spontaneously* breaks the space group

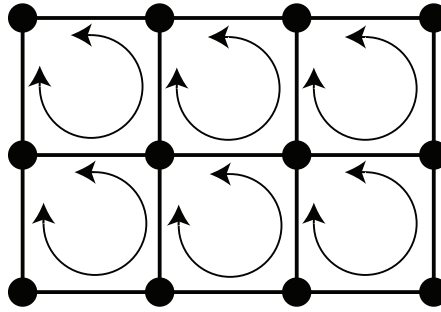


Fig. 5. A schematic representation of the model H_s with additional ring exchange couplings which are tuned by the value of g . Unlike Fig 1, all couplings have the full square lattice symmetry.

symmetry of the square lattice. A specific example of such a VBS state is given by the columnar state of Fig. 6.

Remarkably, we have argued,² it is possible to have a direct second order phase transition between these two phases. This is the first sign of the breakdown of the LGW paradigm. The two phases break distinct spin rotation and lattice symmetries, and LGW theory predicts¹⁶ that such states cannot generically be separated by a continuous phase transition. The theory of Senthil *et al.*² shows that there is indeed a complete breakdown of the basic ideas of the LGW paradigm and an essentially new description is needed of the critical singularities. This description involves ‘deconfined’ fractionalized degrees of freedom in a precise sense - hence the terminology ‘deconfined quantum critical points’.

Consider then spin-1/2 models which preserve all the symmetries of the underlying square lattice in the class

$$H_s = J \sum_{\langle ij \rangle} \mathbf{S}_i \cdot \mathbf{S}_j + \dots \quad (3.1)$$

Here J is a nearest-neighbor antiferromagnetic exchange and takes equal values between all nearest neighbors. The ellipses represent further short-range exchange interactions (possibly involving multiple spin ring exchange) which preserve the full symmetry of the square lattice. (The model H_d is a member of the class H_s only at $g = 1$). Here we will continue to denote by g the strength of these additional non-nearest neighbor couplings that preserve the square lattice symmetry: an example is shown in Fig 5.

A sketch of a section of the phase diagram of H_s , along with possible VBS orders in the $g > g_c$ paramagnet for $S = 1/2$, is shown in Fig 6. Note that the VBS wavefunction is actually similar to the simple coupled dimer wavefunction in Fig 2. However, because of the absence of dimerization in the underlying Hamiltonian, this ground state is at least four-fold degenerate. The choice among these states leads to a particular pattern in the modulation of the exchange energies of the bonds, and a breaking of the spatial symmetries of the square lattice.

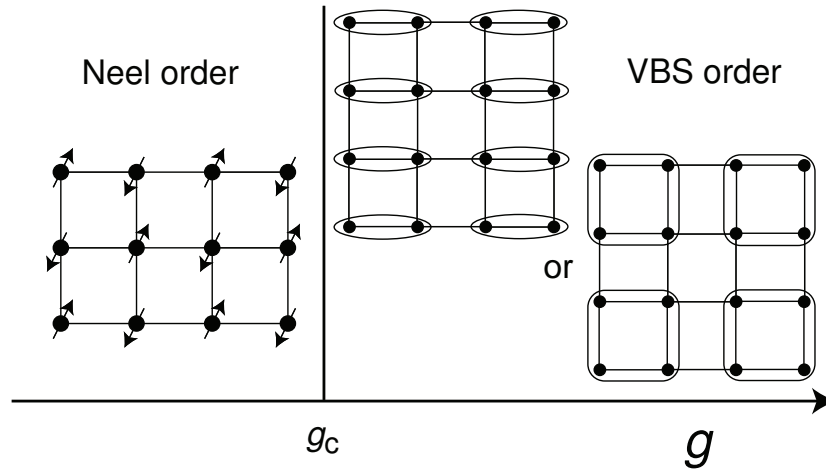


Fig. 6. Phase diagram of H_s for $S = 1/2$. Unlike the paramagnet in Fig 4, the paramagnet here has spontaneous VBS order because all bonds are equivalent in the Hamiltonian, and its ground state breaks spatial lattice symmetries. The spinful excitations of the paramagnets in Figs 4 and above are however similar, and both obey Eq. (1.3).

In the absence of these additional couplings, it is clear that H_s has a conventional Néel ground state with the order parameter defined in Eq. (2.7) obeying $\langle \varphi_\alpha \rangle \neq 0$. Increasing the value of g is expected to enhance the quantum fluctuations about such a state, and we attempt to describe this by setting up a coherent state path integral over the time histories of the spins. In doing this, it is essential to carefully account for the Berry phases of the spins, something we circumvented in our discussion in Section 2. Explicitly, the time evolution of each spin contributes a phase factor to the path integral given by

$$\exp\left(iS \times (\text{oriented area enclosed by trajectory of spin on the unit sphere})\right),$$

where $S = 1/2$ is the angular momentum of each spin; see Fig 7. Fortunately, the role of these Berry phases has been elucidated before in the work of Haldane,¹⁷ and Read and Sachdev,^{18,19} and the subtle summation over the oscillating Berry phases in Fig 7 is reviewed elsewhere.¹⁰ Here we recap the physical picture that emerges from these studies. First, the Berry phases have been shown to play an unimportant role for all configurations associated with *smooth* changes of the Néel vector field. However they are non-vanishing once we allow for singular ‘hedgehog’ or monopole configurations of the Néel field in space-time. These monopoles correspond (in the quantum system) to tunnelling events which involve a change in the skyrmion number, \mathcal{Q} , of the spin configuration (see Eq. (1.5)). Of crucial importance is the result that, due to the Berry phases, the skyrmion-number changing operator (which corresponds to the monopole in the path integral) transforms non-trivially under square lattice translations and rotations. As usual, the statistical weight in the partition function must respect the symme-

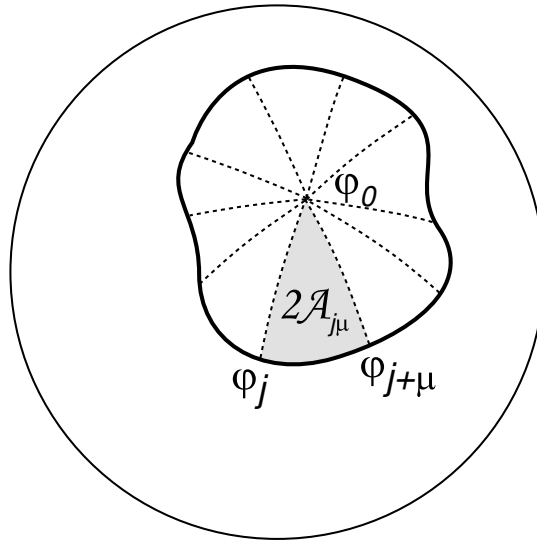


Fig. 7. Computation of the spin Berry phases. It is useful to discretize spacetime into a cubic lattice of points j , and define the orientation of the spin at each j by a unit vector $\varphi_{j\alpha}$ times the sublattice staggering factor η_j in Eq. (2.7). Also define $\mathcal{A}_{j\mu} = (1/2) \times (\text{oriented area of triangle formed by } \varphi_{j\alpha}, \varphi_{j+\mu,\alpha} \text{ and an arbitrary reference point } \varphi_{0,\alpha})$; here $\mu = \tau, x, y$. Then the Berry phase contribution of all the spins is $\exp\left(i2S \sum_j \eta_j \mathcal{A}_{j\tau}\right)$.

tries of the problem. This implies that (for S not an even integer) the fugacity for single monopoles oscillates with a particular pattern (with zero average) on the lattice. Indeed, for $S = 1/2$ the “lowest” skyrmion number-changing event with a non-oscillating fugacity occurs for “quadrupled” processes in which $\Delta\mathcal{Q} = \pm 4$. The coincidence of this factor of 4 and the 4-fold degeneracy of the VBS ground states is not accidental (see below).

Now consider the description of the phases of the spin Hamiltonian. In the Néel phase the monopole events are clearly suppressed at low energies. However, in the paramagnet (the ‘quantum disordered state of the Néel magnet’) the space-time configurations of the Néel field must be riddled with monopoles. In other words, we may think of the paramagnet as having a ‘condensation’ of the skyrmion number changing operator. Now the non-trivial transformation of this operator under lattice symmetry operations (which is due to the Berry phases) leads to broken lattice symmetry in the paramagnet - this may then be identified as VBS order.

Note the dual role played by the monopole configurations. When they proliferate Néel order cannot survive. At the same time their proliferation induces broken translation symmetry. Actually although we haven’t explained it here, it can be shown that the monopoles play a third, equally important, role. Their proliferation leads to confinement of any $S = 1/2$ quanta into integer spin excitations. A similar confinement was illustrated in Fig 3b for the coupled dimer model, but here the ‘string tension’ of the confining potential is provided by the spontaneous VBS order, rather than the modulation of bond strengths in the Hamiltonian.

The lowest lying confined $S = 1$ excitation forms a triplon particle which contributes to a χ_φ of the form in Eq. (1.3).

In our work,² we argued that a direct second order transition is possible between these two phases, and that the monopoles are asymptotically absent at long length and time scales at the critical point. (More precisely, the oscillating single-monopole fugacities average to zero in the continuum limit, and the remaining *quadrupled* monopole fugacity renormalizes to zero at the critical fixed point). We dubbed this a deconfined quantum critical point. The absence of monopoles at the critical fixed point has the immediate consequence that the skyrmion number \mathcal{Q} is *conserved*. This is an extra topological conservation law that is a special property of the deconfined quantum critical point. It does not obtain away from the critical point in either phase. It also does not hold at the conventional O(3) fixed point that describes the transitions of Section 2. It thus provides a sharp distinction between the deconfined critical point and the more conventional LGW theory \mathcal{S}_φ in Eqn. 2.4.

Note that the absence of monopoles at the deconfined fixed point suggests that spin-1/2 spinons get “liberated” right at the critical point (after all, it is the proliferation of the monopoles in the paramagnet that confines the spinons). More detailed considerations led to the proposal² that the deconfined critical point is described by the following critical theory of the fractionalized $S = 1/2$ z_a quanta coupled to a non-compact U(1) gauge field A_μ :

$$\begin{aligned} \mathcal{Z}_{\text{deconfined}} &= \int \mathcal{D}z_a(r, \tau) \mathcal{D}A_\mu(r, \tau) \\ &\times \exp\left(-\int d^2r d\tau \left[|(\partial_\mu - iA_\mu)z_a|^2 + s|z_a|^2 \right. \right. \\ &\quad \left. \left. + \frac{u}{2}(|z_a|^2)^2 + \frac{1}{2e^2}(\epsilon_{\mu\nu\lambda}\partial_\nu A_\lambda)^2 \right] \right). \end{aligned} \quad (3.2)$$

Here z is a two-component spin-1/2 complex spinor. The parameter s is tuned by varying g , and its value must be adjusted so that $\mathcal{Z}_{\text{deconfined}}$ is at its own critical point. The gauge field A_μ is closely related to the compact field \mathcal{A}_μ defined in Fig 7, but it becomes effectively non-compact in the continuum limit appropriate to the critical point.

The Néel vector field is a composite of the spinon fields

$$\vec{\varphi} = z^\dagger \vec{\sigma} z \quad (3.3)$$

This is just the well-known CP^1 representation of the unit vector $\vec{\varphi}$. However, it is absolutely crucial that the gauge field A_μ be regarded as *non-compact*. Indeed, it is the non-compactness that allows for the conservation of the skyrmion number that obtains at the critical point. To see this, note that we can also express⁶ the conserved \mathcal{Q} as

$$\mathcal{Q} = \frac{1}{2\pi} \int dx dy (\partial_x A_y - \partial_y A_x), \quad (3.4)$$

and it is evident that this is strictly conserved by $\mathcal{Z}_{\text{deconfined}}$ so long as the gauge field is non-compact. In contrast for a compact gauge theory, instanton events which change the gauge flux by 2π are allowed which then kills the conservation of \mathcal{Q} . It should now be clear that these instanton events precisely describe the skyrmion-number changing monopoles.

How are we to reconcile the absence of monopoles at the critical fixed point with their supposed proliferation in the paramagnetic phase? The answer is that although (in the presence of appropriate Berry phases) monopoles are irrelevant at the critical fixed point of $\mathcal{Z}_{\text{deconfined}}$, they are *relevant* at the paramagnetic fixed point of this theory. Indeed the paramagnetic phase of $\mathcal{Z}_{\text{deconfined}}$ is aptly described as a U(1) spin liquid²⁰ with a gapless deconfined ‘photon’ field A_μ . This is *unstable* to the inclusion of monopoles (unlike the critical fixed point). The resulting flows away from this U(1) spin liquid lead to the VBS phase with broken translation symmetry, and confined spinons. The structure of the renormalization group flows is shown in Fig. 8 (a similar structure of flows was discussed earlier^{5,19,21} for SU(N) quantum antiferromagnets for large N). Unlike the usual O(n) fixed point of Eq. (2.4), here the initial flow away from the critical fixed point is not toward a stable paramagnet but rather toward the unstable U(1) spin liquid state.

Renormalization group flows with this structure have the general consequence of having two distinct diverging length or time scales (or equivalently two vanishing energy scales). Consider the paramagnetic side close to the transition. First there is the spin correlation length ξ whose divergence is described by $\mathcal{Z}_{\text{deconfined}}$. At this scale there is a crossover from the critical fixed point to the unstable paramagnetic U(1) spin liquid fixed point which has the free photon. However the instability of this spin liquid fixed point to VBS order and confinement occurs at a much larger scale ξ_{VBS} which diverges as a power of ξ .

The physical consequences of the existence of such a deconfined critical point have been discussed in detail in our work.² Here we simply make a few brief further clarifying observations. One immediate consequence of the emergent topological conservation law is that it fixes the scaling dimension of the flux density (or Néel skyrmion density in terms of the spin variables) operator $f_0 = (\partial_x A_y - \partial_y A_x)$. At criticality, this conservation law implies $\langle f_0(R)f_0(0) \rangle \sim R^{-4}$ at long distances. Furthermore, slightly away from the critical point this conservation of skyrmion number holds only up to the length scale ξ_{VBS} which diverges faster than the spin correlation length. The resulting structure of correlations close to the critical point (on the VBS side) is shown in Fig 9, and discussed in detail in our work.² As usual, quantum critical correlations obtain for length scales R much smaller than the correlation length ($R \ll \xi$), where for example spin-spin correlations show power law decay, while the flux correlations have the R^{-4} form described earlier. At intermediate length scale $\xi \ll R \ll \xi_{VBS}$, the spin-spin correlators fall off exponentially, but the flux density correlators are power law but now decay as R^{-3} which is characteristic of flux correlations in the presence

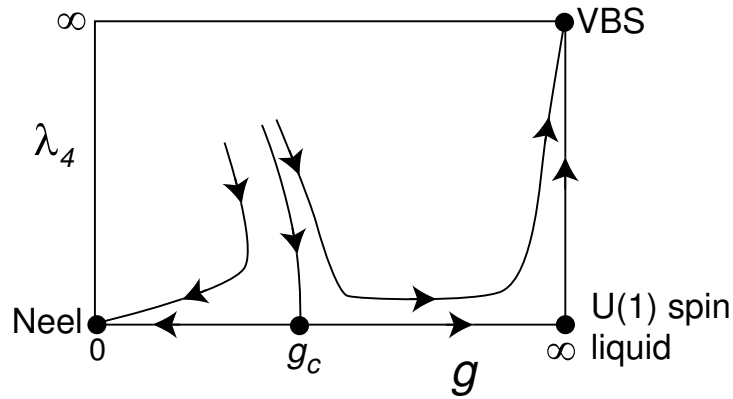


Fig. 8. Schematic renormalization group flows for the $S = 1/2$ square lattice quantum antiferromagnet H_s in Eq. (3.1). The theory $\mathcal{Z}_{\text{deconfined}}$ in Eq. (3.2) describes only the line $\lambda_4 = 0$ (with $s \sim (g - g_c)$): it is therefore a theory for the transition between the Néel state and a U(1) spin liquid with a gapless ‘photon’. However, the lattice antiferromagnet always has a non-zero bare value of the monopole fugacity λ_4 (the monopoles are quadrupled by the Berry phases, as reviewed elsewhere¹⁰). The λ_4 perturbation is irrelevant at the $g = g_c$ critical point of $\mathcal{Z}_{\text{deconfined}}$: this critical point therefore also described the transition in the lattice antiferromagnet. However, the $g \rightarrow \infty$ U(1) spin liquid fixed point is *unstable* to λ_4 , and the paramagnet is therefore a gapped VBS state. In the earlier discussion^{5,19,21} of such flows for large N SU(N) quantum antiferromagnets, the monopoles were found to be irrelevant at the critical point with or without Berry phases, while for $N = 2$, Berry phases are required to render the monopoles irrelevant at criticality. It was this crucial distinction between large and small N which ultimately prevented a complete picture from emerging from the early large N studies.^{5,19,21}

of free photons. Finally at the longest length scales $\xi_{VBS} \ll R$, VBS order is established and the photon is destroyed.

The continuum theory $\mathcal{Z}_{\text{deconfined}}$ has a strongly-coupled critical point, and the remarks made in Section 2 for the critical field theory of \mathcal{S}_φ can be extended to the present situation. The z_a quasiparticles are not well defined at the critical point, and characterized instead by their own anomalous dimension. Indeed, the critical theory of $\mathcal{Z}_{\text{deconfined}}$ may be understood by the usual renormalized perturbative analysis¹ but applied to a theory of nearly free, fractionalized z_a quanta. It is instructive to compute the leading order prediction for the exponent η in Eq. (1.4) in such an approach. At tree level, the z_a propagator is $1/p^2$ (p is a spacetime 3-momentum); the χ_φ susceptibility, by Eq. (3.3), involves the convolution of 2 such propagators, and so we obtain

$$\chi_\varphi(p) \sim \int \frac{d^3 p_1}{p_1^2 (p + p_1)^2} \sim \frac{1}{|p|} \quad (3.5)$$

Comparing with Eq. (1.4), this simple computation yields a large anomalous dimension $\eta = 1$. This illustrates our claimed secondary characteristic of deconfined critical points: the possi-

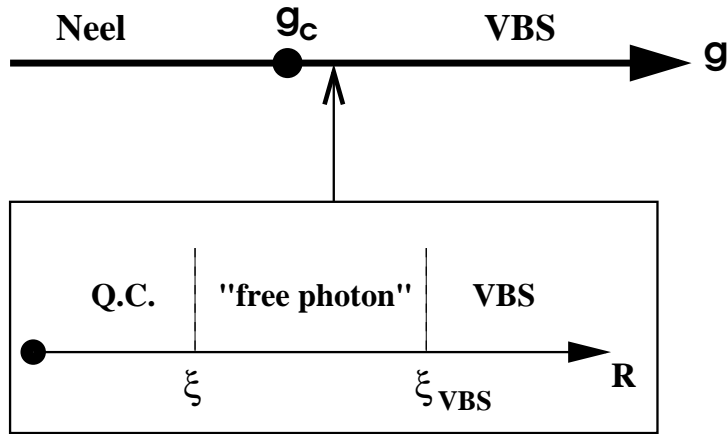


Fig. 9. Structure of correlations on approaching the deconfined Néel-VBS quantum critical point from the VBS side. Two diverging length scales, the correlation length ξ and a longer length scale ξ_{VBS} are present. As usual, at length scales R shorter than ξ , quantum critical (Q.C.) correlations are observed - *e.g.* spin-spin correlators are power law and flux-flux correlators fall off as $\sim R^{-4}$. At intermediate length scales, $\xi \ll R \ll \xi_{VBS}$, spin correlators are exponentially decaying while flux-flux correlators take on the free photon form $\sim R^{-3}$. At the longest length scales, only VBS order is present.

bility of larger values for η .

In view of the crucial role played by the Berry phases in this entire section, it is instructive to ask why they weren't a serious issue in the coupled dimer model considered in Section 2.1. The modulation of the coupling constants in H_d implies that there is a natural pairing of the spins, with each spin having a unique partner on its dimer. This pairing means that the Berry phase terms can be naturally grouped into mutually cancelling terms. At sufficiently large scales the cancelling Berry phases will renormalize to zero, and so their effects can be absorbed into effective values of the real terms in the action; this was implicitly done in writing down the LGW field theory in Eq. (2.4). However, the intermediate length scale over which the Berry phases have not cancelled out is also the scale over which the constituent spinon-structure of the triplon shown in Fig 3b is present. This reasoning makes it clear that the absence of explicit Berry phases in the LGW field theory in Eq. (2.4) implies that this field theory contains no signatures of spinon excitations, which contradicts the central assertion of Bernevig *et al.*⁴

The natural pairing of the Berry phases into mutually cancelling terms clearly does not extend to the model H_s of interest in this section. Each spin has a choice between four nearest neighbor partners, and the choices between different spins are correlated in a highly non-trivial manner. So determining the appropriate cancellations among the Berry phases is a much more delicate matter^{2,10} and leads to the results described above.

Acknowledgments

We are grateful to R. Shankar for valuable discussions and helpful comments on the manuscript. This research was supported by the National Science Foundation under grants DMR-0308945 (T.S.), DMR-9985255 (L.B.), DMR-0098226 (S.S.) and DMR-0210790, PHY-9907949 (M.P.A.F.). We would also like to acknowledge funding from the NEC Corporation (T.S.), the Packard Foundation (L.B.), the Alfred P. Sloan Foundation (T.S., L.B.), a John Simon Guggenheim Foundation fellowship (S.S.), a Pappalardo Fellowship (A.V.) and an award from The Research Corporation (T.S.).

References

- 1) S.-k Ma, *Modern Theory of Critical Phenomena* (W. A. Benjamin, Reading, Mass., 1976).
- 2) T. Senthil, A. Vishwanath, L. Balents, S. Sachdev, and M. P. A. Fisher, *Science* **303**, 1490 (2004);
T. Senthil, L. Balents, S. Sachdev, A. Vishwanath, and M. P. A. Fisher, *Phys. Rev. B* **70**, 144407 (2004).
- 3) R. B. Laughlin, *Adv. Phys.* **47**, 943 (1998); *Science* **303**, 1475 (2004).
- 4) B. A. Bernevig, D. Giuliano, and R. B. Laughlin, *Annals of Physics* **311**, 182 (2004).
- 5) A. V. Chubukov, S. Sachdev, and J. Ye, *Phys. Rev. B* **49**, 11919 (1994).
- 6) R. Rajaraman, *Solitons and Instantons* (North Holland, Amsterdam, 1982).
- 7) K. Chen, A. M. Ferrenberg, and D. P. Landau, *Phys. Rev. B* **48**, 3249 (1993).
- 8) M. Matsumoto, C. Yasuda, S. Todo, and H. Takayama, *Phys. Rev. B* **65**, 014407 (2002).
- 9) M. P. Gelfand, R. R. P. Singh, and D. A. Huse, *Phys. Rev. B* **40**, 10801 (1989).
- 10) S. Sachdev, in *Quantum magnetism*, U. Schollwöck, J. Richter, D. J. J. Farnell and R. A. Bishop eds., *Lecture Notes in Physics*, Springer, Berlin (2004), cond-mat/0401041.
- 11) N. Cavadini, G. Heigold, W. Henggeler, A. Furrer, H.-U. Güdel, K. Krämer and H. Mutka, *Phys. Rev. B* **63**, 172414 (2001).
- 12) M. Matsumoto, B. Normand, T. M. Rice, and M. Sigrist, *Phys. Rev. Lett.* **89**, 077203 (2002) and *Phys. Rev. B* **69**, 054423 (2004).
- 13) A. Oosawa, M. Fujisawa, T. Osakabe, K. Kakurai, and H. Tanaka, *J. Phys. Soc. Jpn* **72**, 1026 (2003).
- 14) D. Yoshioka, G. Arakawa, I. Ichinose, and T. Matsui, cond-mat/0404427.
- 15) K. P. Schmidt and G. S. Uhrig, *Phys. Rev. Lett.* **90**, 227204 (2003).
- 16) For a review see A. Aharony, cond-mat/0201576.
- 17) F. D. M. Haldane, *Phys. Rev. Lett.* **61**, 1029 (1988).
- 18) N. Read and S. Sachdev, *Phys. Rev. Lett.* **62**, 1694 (1989).
- 19) N. Read and S. Sachdev, *Phys. Rev. B* **42**, 4568 (1990).
- 20) The bosonic spinon U(1) spin liquid state appearing here should be distinguished from the U(1) “staggered flux” spin liquid, which is described in terms of gapless fermionic spinon excitations. It has been argued in M. Hermele, T. Senthil, M. P. A. Fisher, P. A. Lee, N. Nagaosa, and X. - G. Wen, cond-mat/0404751 that, at least for large N SU(N) antiferromagnets, the staggered flux spin liquid is stable against proliferation of monopoles. The monopole fugacity can be an irrelevant perturbation to the staggered flux spin liquid due to the presence of gapless spinon excitations. In this sense, the staggered flux spin liquid *phase* is similar to the $g = g_c$ critical fixed *point* of Fig 8. The U(1) spin liquid phase of Fig 8 is controlled by the $g = \infty$ fixed point: this has only has gapped spinon excitations, monopoles are relevant, and so the entire $g > g_c$ spin liquid phase is unstable.
- 21) G. Murthy and S. Sachdev, *Nucl. Phys. B* **344**, 557 (1990).